Journal of Structural Biology **125,** 25–38 (1999)
Article ID jsbi.1998.4061, available online at http://www.idealibrary.com on IDEAL®

Effects of Surface-Bound Water and Surface Stereochemistry on Cell Adhesion to Crystal Surfaces

Ella Zimmerman,* Lia Addadi,* and Benjamin Geiger†

**Department of Structural Biology and †Department of Molecular Cell Biology, The Weizmann Institute of Science, 76100 Rehovot, Israel*

Received August 14, 1998

Crystals of calcium-(*R*,*S*)-tartrate trihydrate were used as adhesion substrates (for A6 epithelial cells), to study specific stages in cell adhesion. Events such as surface recognition, cell attachment, spreading, motility, cell–cell aggregation, and cell penetration into the crystal bulk are all shown to depend on the molecular structure of the various crystal faces. These crystals exhibit three chemically equivalent, yet structurally distinct, faces. On the {100}, a layered surface exposing bound water, the cells attach, are motile, and tend to form multicellular aggregates, but do not spread and do not form focal contacts. Following prolonged incubation, single cells attached to the {100} surface undergo apoptosis, while those interacting with other cells are rescued. Macroscopic spiral dislocations emerging on the {100} face of the crystal are highly adhesive for cells. Cells attached to these sites develop long protrusions that penetrate into the crystal. The {011} faces expose mainly hydroxyls attached to the chiral carbons. The cells interact extensively with these faces, are immobilized, do not spread, do not form focal contacts, and subsequently die. The faces belonging to the {0*kl*} family are characterized by molecular and topographical steps. The cells attach to these faces, spread, and form focal contacts and stress fibers. Thus the molecular character of the crystal surfaces, including the presence of bound water, the exposure of determinants that promote rapid surface recognition, and the effective association with extracellular adhesive proteins, affect the patterns of cell adhesive behavior and fate. © 1999 Academic Press

Key Words: **cell adhesion; cell motility; crystalline water; crystal surfaces; hydration; stereochemistry.**

INTRODUCTION

The adhesion of cells to one another and to the extracellular matrix (ECM)[1] plays a central and essential role in the assembly of multicellular organisms. Such adhesions occur via highly specialized and complex cellular structures such as intercellular junctions (Takeichi, 1995) and cell–ECM adhesions (Geiger *et al.*, 1995; Yamada and Geiger, 1997). These multimolecular assemblies consist of specific transmembrane "adhesion receptors," networks of anchor proteins that link the cytoskeleton to the inner aspects of the plasma membrane, and cytoskeletal elements. In addition to the adhesion molecules, physically mediating the contacts between the external surfaces and the cytoskeleton, these adhesion sites also contain a wide variety of signaling molecules that are involved in long-range adhesion-triggered events.

The assembly of cell–substrate adhesions is commonly viewed as a multistage process, which involves several distinct sequential events, including surface recognition by the cell, formation of initial cell–substrate contacts and their development into focal contacts, followed by cell spreading on the substrate. The maturation of focal contacts involves interactions of integrin receptors with RGD-containing ECM molecules, their clustering, and the formation of cytoskeletal interactions. However, on purely statistical grounds, it appears unlikely that integrin-mediated interactions are directly involved in the initial stages of surface recognition, as the probability of integrin molecules on the surface of a suspended cell to "hit the target" on the ECM is extremely low. These considerations are corroborated by experimental evidence suggesting that integrin-mediated contacts are preceded by earlier events that support and promote the subsequent assembly of integrin-mediated focal contacts. The earlier events consist of multiple cooperative interactions between abundant adhesive components on the cell surface and on the substrate (Hanein *et al.*, 1995). A good

[1] Abbreviations used: CPD, critical point dryer; DAPI, 4,6-diamidino-2-phenylindole; DMEM, Dulbecco's minimum essential medium; ECM, extracellular matrix; EGTA, ethylene glycol-bis(β-aminoethyl ether)*N*,*N*,*N*′,*N*′-tetraacetic acid; MES, 2-[*N*-morpholino]ethanesulfonic acid; PBS, phosphate-buffered saline; SEM, scanning electron microscopy; TEM, transmission electron microscopy.

1047-8477/99 $30.00
Copyright © 1999 by Academic Press
All rights of reproduction in any form reserved.

example for such interactions is the anchoring of leukocytes to the vascular wall first via selectins and then via integrins (Butcher and Picker 1996; Kansas, 1996; Springer, 1994). In other systems, however, the molecular properties of these early interactions, including the nature of the components on the cell membrane and on the external surface, are still poorly defined.

The use of crystals as adhesion substrates (Hanein *et al.*, 1993b, 1994, 1995, 1996) provided a unique opportunity to test the specificity of cell substrate recognition, define specific phases in the adhesion process, and characterize them at the molecular level. The results of the studies performed on calcium-(*R*,*R*)-tartrate tetrahydrate and calcium-(*S*,*S*)-tartrate tetrahydrate crystals highlighted the importance of the molecular structure of the substrate and the existence of a highly specific stereoselective recognition mechanism. It was also noted that excessive interactions at the early recognition stage may immobilize the cells on the surface and prevent them from proceeding to integrin-mediated adhesion. Such an exaggerated attachment was thus not followed by cell spreading and did not support long-term cell survival.

The study of cell behavior upon adhesion to each of the different faces of calcium-(*R*,*S*)-tartrate trihydrate crystals, reported here, enabled us to characterize the involvement of specific structural parameters of the substrate in the establishment and development of specific forms of adhesion. In particular, the roles played by substrate-bound water molecules, surface stereochemistry, and surface topography in the attachment of the cells were examined. The results indicate that cell adhesion is controlled by a wide range of interactions and is affected by chemical and topographical variations ranging in size from angstroms to micrometers.

MATERIALS AND METHODS

Crystallization. Optimal conditions for crystallization of calcium-(*R*,*S*)-tartrate trihydrate were determined, ensuring that the crystals were well formed, homogeneous, and reproducible with respect to morphology and size. A solution of 10 ml of 72 mM *meso*-tartaric acid, pH 8.0 (adjusted with 0.4 M NaOH) (Sigma Chemical Co., St. Louis, MO), was mixed with 10 ml of 72 mM $CaCl_2 \cdot 2H_2O$ (Merck-Schuchardt, Darmstadt, Germany) and brought to a final volume of 40 ml. All solutions were slightly preheated and kept warm until poured. The solution was divided into 35-mm tissue culture dishes (Falcon, Becton Dickinson Labware, Plymouth, UK) either containing or not containing glass coverslips (Smethwick, Warley, England), at room temperature. Typically, crystals of 100–200 μm in length form within 1 day and remain attached to the dish or glass surface. The morphology of typical crystals was determined by x-ray diffraction on a CAD-4 diffractometer (Enraf-Nonius, Philips, Eindhoven, Holland) and with a scanning electron microscope (Jeol, JSM-6400, Jeol Ltd., Tokyo, Japan).

Cell culture. A6 cells (*Xenopus laevis*, epithelial kidney cells, ATCC CCL 102) were cultured at 27°C in Dulbecco's minimum essential medium (DMEM, Biological Services, the Weizmann Institute) supplemented with 10% fetal calf serum (Biolab Lab. Ltd., Jerusalem, Israel), in a humidified atmosphere of 5% CO_2 in air.

Crystals that were previously grown on either glass slides or tissue culture dishes were sterilized under UV light for 2 h and A6 cells were seeded. To avoid crystal dissolution during incubation with the cells and later treatments, all media, fixation, antibodies, and washing solutions were saturated with calcium-(*R*,*S*)-tartrate trihydrate crystals. The saturation procedure consisted of overnight incubation of excess crystals with the relevant solution and filtering it before use. Cells to be seeded on the crystals were suspended with trypsin versene, centrifuged, resuspended in the saturated medium, and seeded on the crystals. Crystal-attached cells were monitored by optical microscopy and serial photographs were taken at different time points.

Scanning electron microscopy (SEM). Crystal–cell samples on glass slides were fixed with 2% glutaraldehyde in 0.1 M cacodylate buffer containing 5 mM $CaCl_2$, pH 7.2, for 30 min. The glass slides were rinsed three times, for 5 min each, with 0.1 M cacodylate buffer and postfixed for 1 h with 1% osmium tetraoxide in 0.1 M cacodylate buffer. The slides were rinsed, dehydrated with ethanol, and critical point dried with CO_2 (Pelco CPD2, Ted Pella, Inc., Redding, CA). The glass slides were placed on carbon-coated stubs (Spi Supplies, West Chester, PA), using silver paste, and sputter coated with gold for 6 min at 8 mA followed by 6 min at 10 mA (S150 Edwards, Sussex, UK). The specimens were examined with the scanning electron microscope operated at 20 kV.

Transmission electron microscopy (TEM). Crystal–cell samples on tissue culture dishes were fixed for 1 h with 2% glutaraldehyde and 1% paraformaldehyde (Spi Supplies) in 0.1 M cacodylate buffer, 5 mM $CaCl_2$, pH 7.2. The specimens were rinsed four times, embedded in a thin layer ($<$1 mm) of 1.6% agar and 1% gelatin, and fixed as above for 4 h. After additional rinsing the cells were postfixed with 1% osmium tetraoxide, 0.5% potassium ferrocyanide, and 0.5% potassium dichromate in 0.1 M cacodylate buffer, pH 7.2, followed by four washings with water. The crystals were then dissolved with 0.2 M EGTA, pH 7.2, overnight. The cells were stained *en bloc* with 2% aqueous uranyl acetate (1 h) followed by ethanol dehydration. The specimens were embedded in t-Epon 812 (Tuosimis, MD). Sections of 500–700 Å were cut using a diamond knife (Diatome, Biel, Switzerland) and placed on copper grids. The sections were stained with uranyl acetate and lead citrate and examined in Philips EM410 TEM at an accelerating voltage of 80 kV.

Fluorescence microscopy. Cells seeded on glass coverslips that had attached crystals were rinsed once with MES buffer, pH 6.0, permeabilized by incubation with 0.5% Triton X-100 (in the MES buffer) for 2 min, and fixed for 25 min with 3% paraformaldehyde in phosphate-buffered saline (PBS). After several washings with PBS, cells were incubated for 45 min at room temperature with the primary antibody, rinsed three times with PBS, and incubated with the secondary antibody for 45 min. After being rinsed with PBS, specimens were mounted in elvanol (Mowiol 48-8, Heochst, Frankfurt, Germany). Antibodies used included monoclonal anti-human vinculin (hVin, Sigma), anti-Pan-cadherin (CH19, Sigma), anti-paxillin (Transduction Laboratories, Lexington, KY). Secondary antibodies were Cy3-labeled goat anti-mouse IgG (Jackson ImmunoResearch Labs, Inc., West Grove, PA).

To visualize nuclei, after fixation was completed as described above, cells were labeled with DNA-specific dye (DAPI, 4,6-diamidino-2-phenylindole; Sigma) for 40 min, washed several times, and embedded in elvanol. The cells were examined using either a Zeiss Axiophot fluorescence microscope (Zeiss, Oberkochen, Germany) equipped with the proper filters or a laser

scanning confocal microscope (MRC-1024, Bio-Rad, Hertfordshire, UK).

Inhibition of adhesion with synthetic RGD peptides. To test the specificity of cell binding to the crystal, the plating medium was mixed with 50 μg/ml synthetic peptide with the sequence Gly-Arg-Gly-Asp-Ser (RGD peptide) or a control peptide Gly-Arg-Gly-Glu-Ser (RGE). Both peptides were synthesized by the peptide synthesis unit of the Weizmann Institute and purified by high-pressure liquid chromatography. The adhesion assay was performed for 1 h.

RESULTS

Calcium meso-Tartrate Trihydrate Crystals

Calcium-(*R*,*S*)-tartrate (or calcium *meso*-tartrate) crystallizes as a trihydrate of known structure (DeVries and Kroon, 1984) (monoclinic $P2\ 1/c$ $P21/c$,$a = 8.921$ Å, $b = 10.300$ Å, $c = 9.881$ Å, $\beta = 91.78°$, $z = 4$).

The determination of the crystal morphology, including the exact indices of the faces, was first performed by x-ray diffraction. Once the basic plate morphology is identified, the angles between each pair of lateral faces, measured by observation under the scanning electron microscope in the appropriate orientations, are sufficient to define the particular morphology of each given crystal.

Under the established growing conditions, the crystals form as irregular platelets (Fig. 1) delimited by prominent plate faces {100}[2] and side faces {011}. Often, faces from the {0*kl*} family were developed with different indices.

The presence of emerging spiral dislocations is prominent on the {100} plate faces (Fig. 1). Complex multicrystalline ensembles originate from these imperfections during crystal growth, forming steps that expose different crystal planes.

On the {100} faces (Fig. 2a), the water molecules (blue) form bilayers parallel to the {100} planes. Parallel to the water bilayer are rows of carboxylate groups (red) of tartrate molecules related by translation and rows of calcium ions (green). The {100} faces may thus expose to the environment either a water layer or a carboxylate/calcium layer. However, in aqueous solution, the water molecules are in excess of at least four orders of magnitude over calcium and tartrate, and thus the face is presumably dominated by water. The macroscopic topography of the face (excluding the imperfection sites) is relatively smooth.

On the {011} faces (Fig. 2b), the bound water molecules are organized in parallel rows, separated by rows of hydroxyl groups of the tartrate molecules

[2] Note: Crystal faces are described by a set of indices (*hkl*) that unequivocally define the orientation of the face relative to the crystallographic axes *a*, *b*, *c* of the structure. The notation {*hkl*} [e.g., {100} and {011} indicates the set of symmetry related faces of identical structure. {0*kl*} represents a set of faces, with $h = 0$.

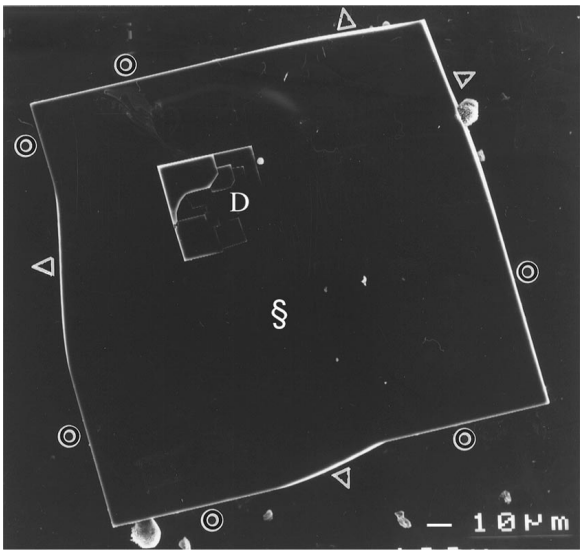

FIG. 1. Scanning electron micrograph of a calcium-(*R*,*S*)-tartrate trihydrate crystal. The different faces are marked as follows: §, (100); ○ (011), Δ, (0*kl*); D, dislocation on the (100) face.

(about 18 Å apart) (red and white). One oxygen atom of one carboxylate group emerges oblique to the surface while the second carboxylate group is almost parallel to it. The overall character of the face is dominated by hydroxyl groups. The face is smooth at the molecular level as well as topographically.

The {0*kl*} faces develop as a set of combinations of faces with different indices. The number and indices of these faces vary among crystals and even within the same crystal. The structure of these faces can vary between different indices. Figure 2c shows the structure of the {023} faces as a representative of the {0*kl*} family. The structure, on these particular faces, is similar to that of the {011} faces yet with larger gaps between the repetitions of the functional groups. The undulation due to the repetition of molecular steps is a dominant characteristic of these faces, while the distance between the steps varies with the index of the face. The surface of these faces is also topographically rough, suggesting that the exposed {0*kl*} faces are an average of combined face directions. The face can thus appear on the average curved, due to a progressive change in the slope at the molecular level (increasing the *h* and *k* indices).

At first approximation, crystals expose to the environment characteristic faces whose structures correspond to that of the bulk, terminated along planes corresponding to the crystallographic directions defined by the crystal morphology. It is important to realize, however, especially in relation to the rough {0*kl*} faces, that the macroscopic direction of a face does not always reveal the microscopic roughness at the nanometer level. There is furthermore a

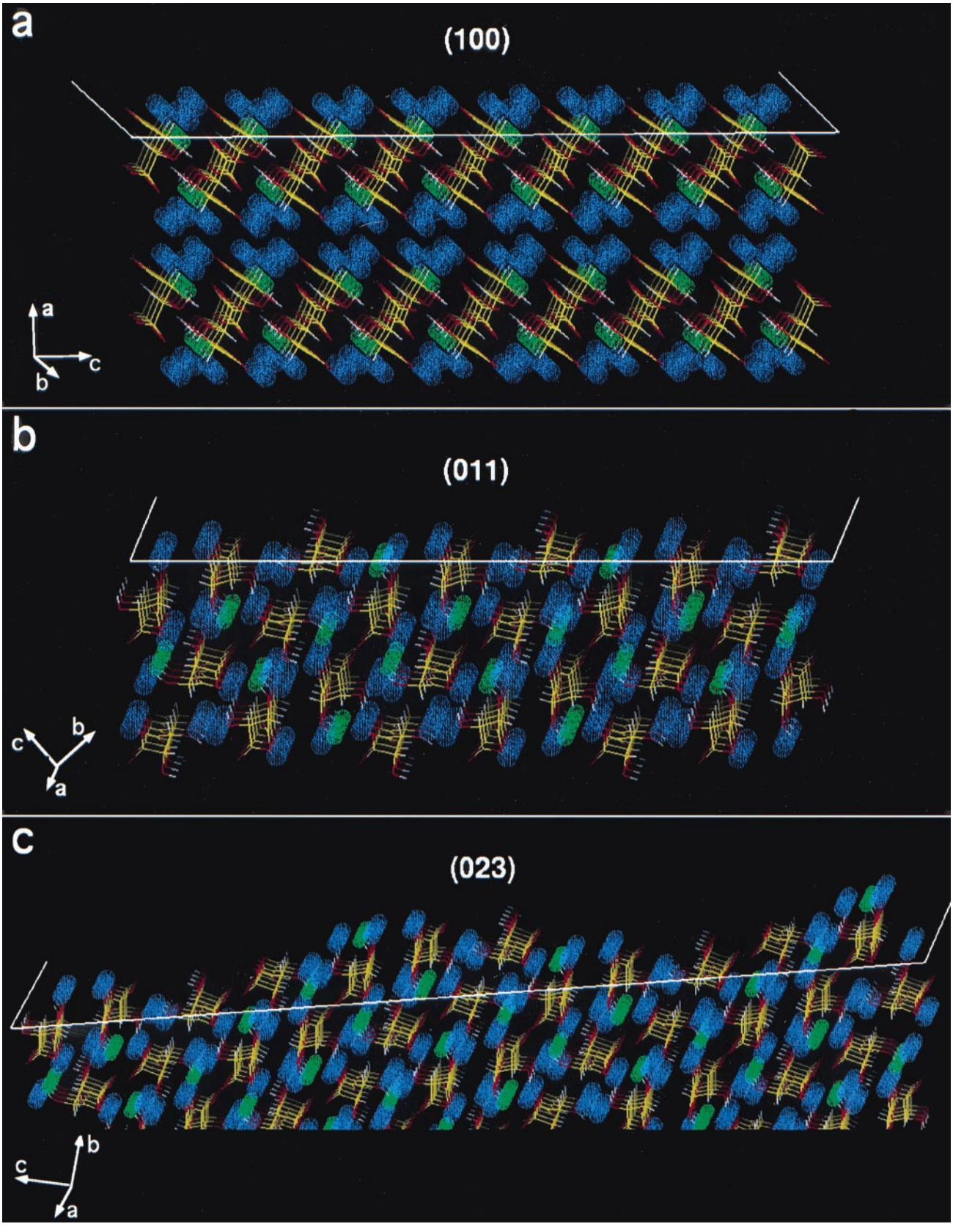

FIG. 2. Packing arrangement of calcium-(*R*,*S*)-tartrate trihydrate crystals on the various developed faces. Calcium ions: green dashed spheres. Water molecules: blue dashed spheres. Tartrate molecular backbone: yellow. Oxygen atoms: red. Hydrogens connected to oxygens in hydroxyl groups: white. The representations are almost edge-on views of the structures. The interface at the top of each structure, defined by white landmarks, represents the plane indicated. (a) (100); (b) (011); and (c) (023) faces. The (023) face is representative of the $\{0kl\}$ family of faces. The directions of the *a*, *b*, and *c* crystallographic axes are indicated.

constant dynamic activity of molecules exchanging at the lattice sites on the crystal surfaces, although the structure is preserved.

Cell Adhesion to the Crystals: Kinetic Features

Cultured epithelial A6 cells were seeded and incubated in complete medium at 27°C on calcium *meso*-tartrate crystals.

The adhesion of the cells to the three face types, {100}, {011}, and {0*kl*}, and their fate are distinctly different. They will thus be described separately for each face. Figure 3 shows an overview of A6 cells on all the face types 6 h after plating. Cells associated with the {100} and {011} faces are mostly spherical while cells on the {0*kl*} faces are well spread. The crystals were grown directly attached to glass cover slips, such that cells attached and spread on the glass substrate provide a convenient control.

To determine the kinetics of cell adhesion to the various faces of calcium-(*R*,*S*)-tartrate trihydrate crystals and to the culture dish, the number of cells attached to the different surfaces at different time points after plating was counted on SEM specimens (Fig. 4). The attachment of the cells to the {011} faces is relatively rapid and massive (~80 cells/mm^2 at 5 min, ~300 cells/mm^2 at 15 min, and ~1200 cells/mm^2 following 1 and 6 h of incubation). Close examination of the {011} faces by scanning electron microscopy following short (5–15 min) incubation with cells revealed numerous cell remnants on the crystal surface (Fig. 5c), suggesting that the cells interact even more intensively at short time intervals with the {011} surface, yet most of these interactions are transient and do not develop into stable adhesions. The cells thus tend to detach, leaving distinctive

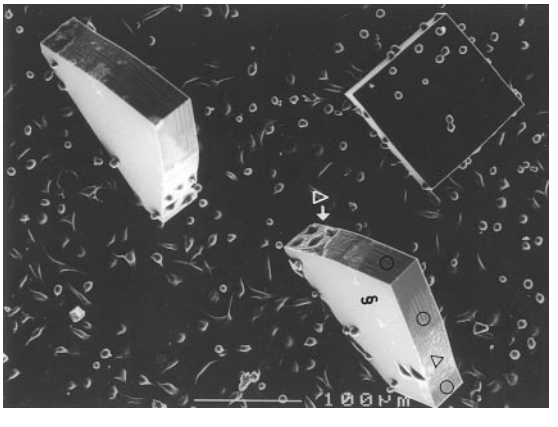

FIG. 3. Scanning electron micrograph of A6 cells plated on calcium-(*R*,*S*)-tartrate trihydrate crystals after 3 h of incubation. The top right crystal lies with its {100} faces parallel to the glass while the top right and bottom crystals have their {100} faces perpendicular to the glass. The faces of the left bottom crystal are marked as in Fig. 1. The cells around the crystals are spread on the glass coverslip.

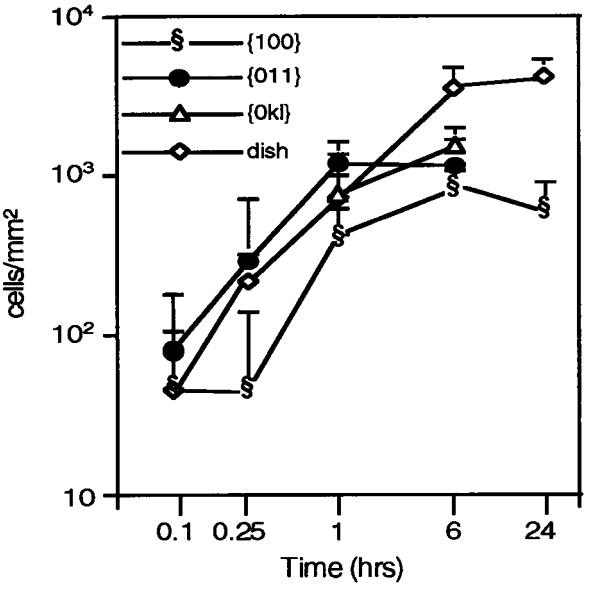

FIG. 4. Number of cells attached to the various faces of calcium-(*R*,*S*)-tartrate trihydrate crystals, after different incubation times. {100} faces (§); {011} faces (●); {0*kl*} faces (Δ); tissue culture dish (◇). The error bars indicate the standard deviation of each data point.

remnants with a diameter matching the size of a single attached cell. After 1 h the process becomes less dynamic, and the cells remain attached to the crystal surface. The initial attachment of A6 cells to the {0*kl*} faces is slower (~750 cells/mm^2 at 1 h of incubation) and the numbers increase with time until confluence is reached (~1600 cells/mm^2). Cell attachment to the {100} faces was detected within several minutes after plating. The number of attached cells was, however, low, around 45 cells/mm^2 at 5–15 min of incubation, and slowly increased to around 400 cells/mm^2 after 1 h of incubation and to 600 cells/mm^2 after 24 h of incubation. On the tissue culture dish the number of cells initially attached was around 45 cells/mm^2 at 5 min of incubation and linearly increased with time to over 4000 cells/mm^2 at 24 h of incubation.

Cell Interactions with the {011} Faces

Scanning electron microscopy indicates that the adherent cells on the {011} faces are initially spherical (Fig. 5a), attached through a foot-like structure, and even after longer incubation (3 h), the cells do not spread (Fig. 5b). Examination of the interface between the cell and the crystal by transmission electron microscopy shows areas with tight adhesions to the surface flanked by areas in which a wide gap between the membrane and the crystal was noted (Fig. 5d).

Immunofluorescence labeling (Fig. 6) of the cells on the {011} faces after 24 h of incubation using

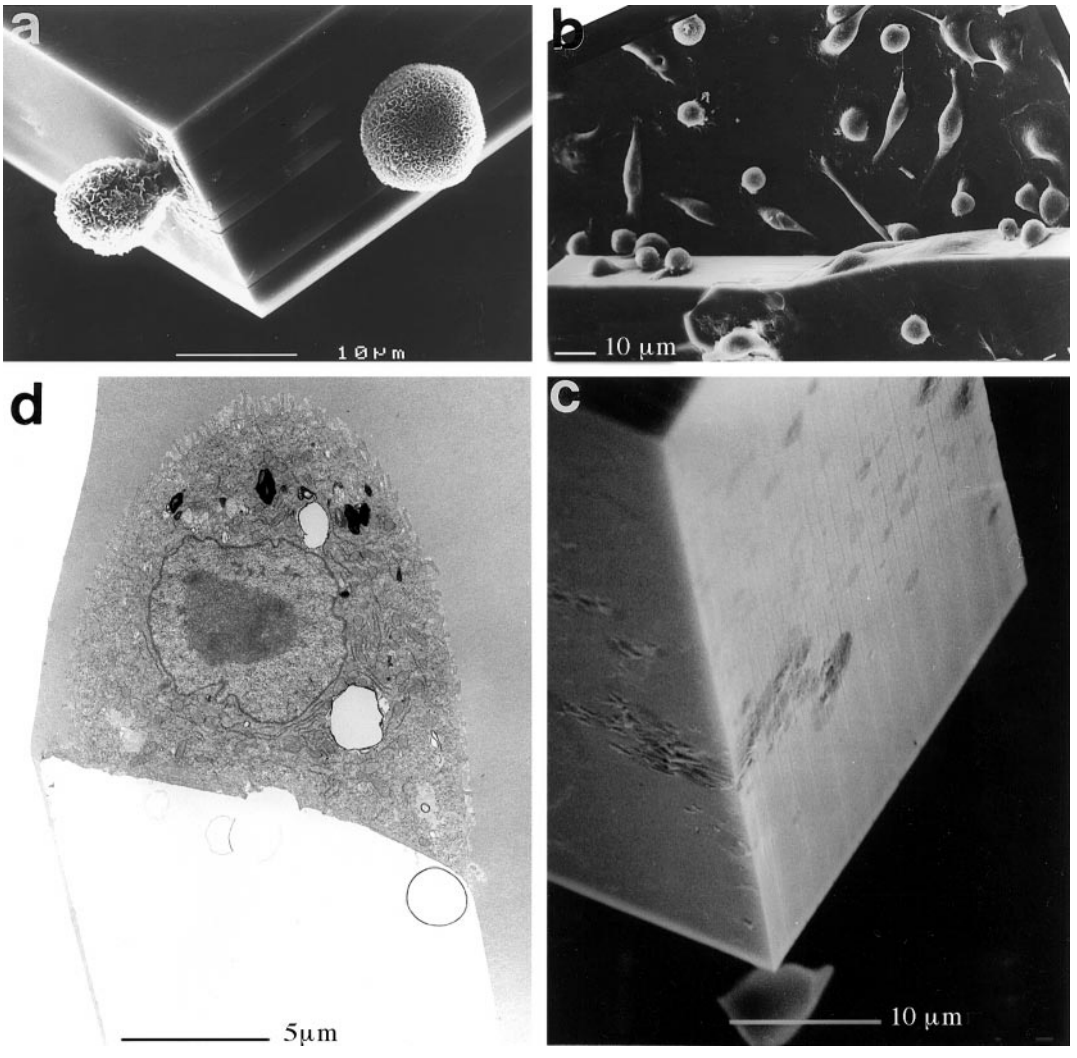

FIG. 5. Scanning (a,b,c) and transmission (d) electron micrographs of A6 cells plated on the {011} faces of calcium-(*R*,*S*)-tartrate trihydrate crystals for various incubation periods: (a) 30 min; (b) 3 h. The (011) crystal face appears at the left and right sides of the picture, interrupted by a stretch of an (0*kl*) face in the middle (where the cells are spread). The cells in the background are attached to the glass coverslip. (c) Cell remnants on a (011) crystal face after a 15-min incubation. (d) Cell attached to the (011) face, following a 24-h incubation. Note that the angles between the crystal faces in this section do not correspond to the dihedral angles between the {100} and the {011} faces due to the direction of sectioning, which is not necessarily perpendicular to the crystal plate.

anti-vinculin and anti-paxillin antibodies gave no evidence for focal contact formation (Fig. 6, (011)), in contrast to cells growing on the culture dish or the glass coverslips (Fig. 6, dish). Observations were made with a laser confocal microscope, to allow visualization of the interface between cell and crystal.

Staining with DAPI indicated that individual cells attached to the {011} faces at 24 h after plating showed, in most cases, fragmented nuclei typical of apoptotic cells (Fig. 7, (011)).

Cell Interaction with the {0kl} faces

In contrast to the cells on the {011} and {100} faces, the cells attached to the {0*kl*} faces spread rapidly and within 1–3 h cover most of the crystal surface. This spreading was considerably faster than that observed on the glass coverslips (Fig. 3) or even the tissue culture dish. The overall morphology of the spread cells observed by SEM (Fig. 8a) and TEM (Fig. 8b) is flat; they display an apical-basolateral polarity when reaching confluence and are usually aligned along the long axis of the face. These cells interact with one another through well-developed junctions (Fig. 8b). Transmission electron microscopy indicated that the interaction with the {0*kl*} faces was mediated by specific regions along the ventral cell surface, presumably corresponding to focal contacts (Fig. 8b).

Addition of 50 µg/ml of a synthetic RGD peptide,

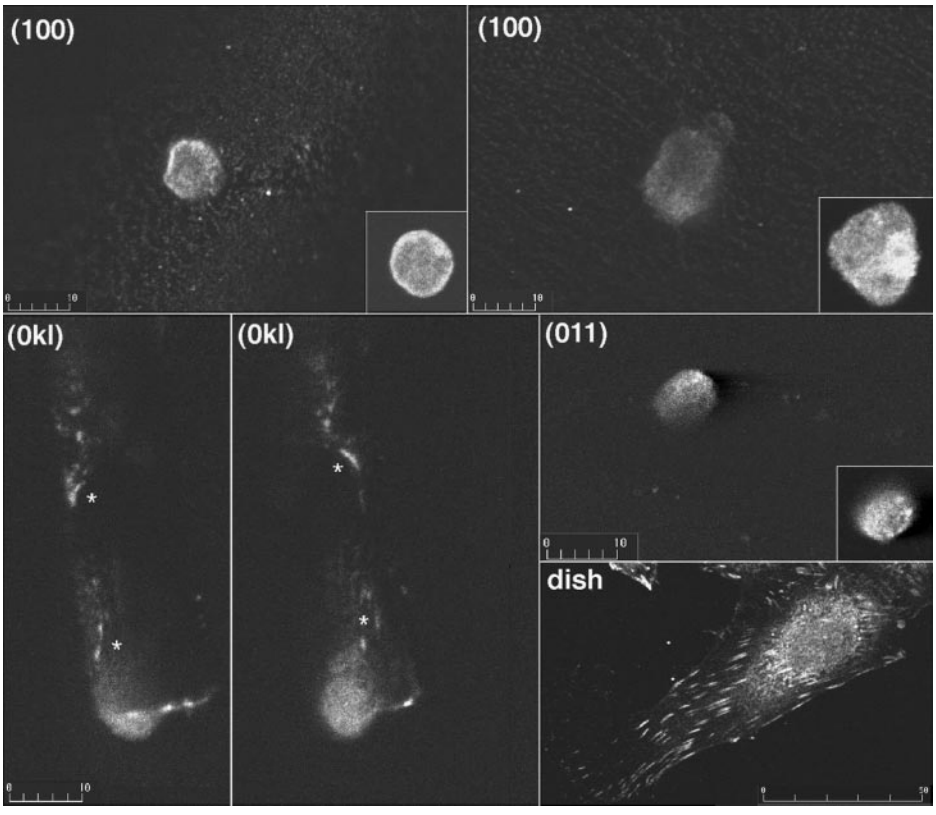

FIG. 6. Confocal immunofluorescence microscopy of A6 cells plated on the different faces of calcium-(*R*,*S*)-tartrate trihydrate crystals after a 24-h incubation and immunolabeling with an antibody against vinculin to visualize focal contacts. (100) (Top left) A single cell viewed at the focal plane of the (100) face. The insert shows the same cell at a higher focal plane away from the crystal surface. (100) (Top right) An aggregate of cells viewed at the focal plane of the (100) face. The insert shows the same aggregate, containing four cells, at a higher focal plane. (0*kl*) (Left and right) Spread cell viewed oblique to the observation plane, on one of the {0*kl*} faces. The asterisks mark typical focal contacts. (011) A single cell attached to a (011) face viewed at the focal plane of the crystal face. (Inset) The same microscopic field viewed at a higher focal plane. (Dish) A well-spread cell attached to the glass coverslip, showing typical focal contacts.

an inhibitor of integrin-mediated interactions of cells with adhesive proteins such as fibronectin and vitronectin, completely inhibited cell adhesion to the {0*kl*} faces (data not shown).

Immunofluorescence staining confirmed that cells spread on the {0*kl*} faces form extensive vinculin-rich focal contacts (Fig. 6, (0*kl*)). The structural organization and size of these focal contacts was by and large similar to that of focal contacts formed by cells growing on glass coverslips (Fig. 6, (0*kl*), dish).

DAPI staining showed that the nuclei of cells attached to the {0*kl*} faces was flat and apparently intact (Fig. 7, (0*kl*)).

Cell Interactions with the {100} Faces

A6 cells attach to the {100} faces (the large plate faces) of calcium-(*R*,*S*)-tartrate crystals, yet they remain mostly spherical even following long (24 h) incubation (Fig. 9b). Occasionally spread cells were observed on the {100} faces (Fig. 3), yet they were usually associated with macroscopic steps on the crystal surface, locally exposing different crystal planes.

Continuous light microscopic monitoring of cells attached to the {100} faces using time-lapse cinematography (Fig. 9a) showed that the cells associated with the crystal surface are highly motile. Following a long incubation time, cells undergo progressive clustering and at 24 h nearly 80% of the cells form multicellular aggregates (Fig. 9a, 24). These aggregates, typically composed of three to eight cells (Fig. 9c), are attached to the surface through one or two cells and retain motile activity. Transmission electron microscopy showed that the cells in these aggregates are tightly associated with one another, while the attachment to the crystal surface is limited and apparently discontinuous (Fig. 9d).

Immunofluorescence staining for vinculin or paxillin indicated that A6 cells do not form focal contacts with the {100} faces, irrespective of whether the cells are single (Fig. 6, (100) left) or in multicellular aggregates (Fig. 6, (100) right). Similarly, staining

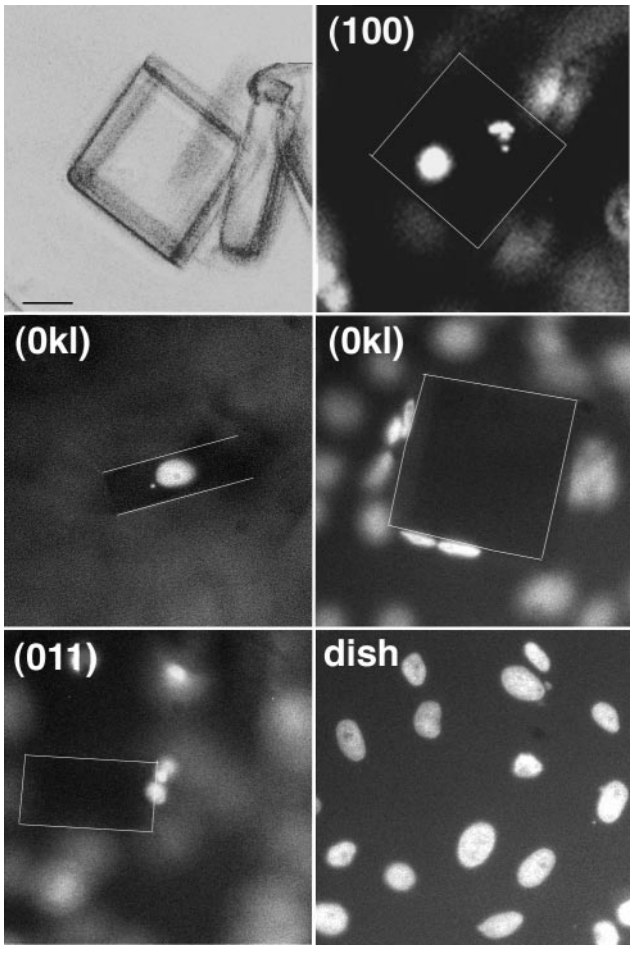

FIG. 7. Fluorescence micrographs of DAPI-stained cells 24 h after plating on the different faces of calcium-(*R*,*S*)-tartrate trihydrate crystals. (Top) Bright-field (left) and DAPI (right) image of a crystal with cells attached to the (100) face. Note one single cell with a fragmented nucleus and a multicellular aggregate with intact nuclei. (0*kl*) Cells attached and spread on {0*kl*} faces, observed face-on (left) and edge-on (right). The nuclei are intact. (011) Two nuclei of two single cells attached to a crystal. The cell attached exclusively to the (011) face is seen edge-on and its nucleus appears fragmented. (Dish) Intact nuclei of well-spread cells on the glass coverslip. Scale bar = 10 μm.

with rhodamine-labeled phalloidin showed no evidence of actin bundle organization in the cells attached to these faces.

Effect of Surface Topography on Cell Interactions with the Crystal Surface

Crystal imperfections (spiral dislocations) on the {100} faces of the calcium-(*R*,*S*)-tartrate trihydrate crystals are highly favorable sites for stable attachment of individual or aggregated A6 cells (Fig. 10a). Scanning electron microscopy shows that following relatively long incubation (24 h), cells have a tendency to reach imperfections on the crystal surface and adhere to them. Transmission electron microscopy of ultrathin sections, cut roughly perpendicular to the {100} plane (Fig. 10b), indicated that cell extensions often penetrate through the imperfections down to at least 7–8 μm into the crystal. This was also confirmed by confocal microscopy using cells stained for vinculin. The original growing dislocations are generally not larger than a few crystal units (nanometers to tens of nanometers), yet in the presence of the penetrating cells they expand to the micrometer range. The width of these dislocations and their depth under the {100} faces strongly suggest that the cells are actively involved in expanding the imperfections. Typically, the penetration of the cells into these structures was mediated by thin processes that were tightly attached to the lateral walls of the grooves. These membrane protrusions either reached the bottom of the groove (Fig. 10d) or were shorter, with extracellular material filling the gap between the tip and the crystal walls (Fig. 10c). The crystal surfaces exposed inside the imperfections are often rough and extended at variable angles, such that it is impossible to define their indices with certainty.

Apoptotic Fate of Cells Attached to the {100} Faces

DAPI staining of the cells remaining on the {100} faces following 24 h of incubation indicated that about 80% of the nuclei of single cells are undergoing progressive fragmentation, typical of apoptotic cells (Fig. 7, (100), cell on the right). Cells in the multicellular aggregates on the {100} faces, on the other hand, were apparently protected from this apoptotic fate, and even after longer periods, over 80% of their nuclei were apparently normal (Fig. 7, (100), cells on the left). These observations suggest that cell–cell adhesion can rescue cells attached to the {100} faces from apoptosis by providing specific survival signals.

DISCUSSION

During the past several years, a series of studies involving cell adhesion to crystal surfaces was carried out, in an attempt to systematically define the structural and chemical characteristics of substrates that influence cell behavior at the different stages of adhesion (Hanein *et al.*, 1993b, 1994, 1995, 1996). Studies on cell adhesion to crystals of calcium-(*R*,*R*)-tartrate and calcium-(*S*,*S*)-tartrate showed that cells are sensitive, in their initial attachment, to the composition of the substrate, its structural organization, and even the stereochemistry of the molecular moieties comprising its surface. In order to study the nature and effect of this high level of recognition by fine-tuning of the cell–substrate interactions, calcium-(*R*,*S*)-tartrate was selected for the present study. This is the minimal possible molecular modification relative to the two previously studied isomers,

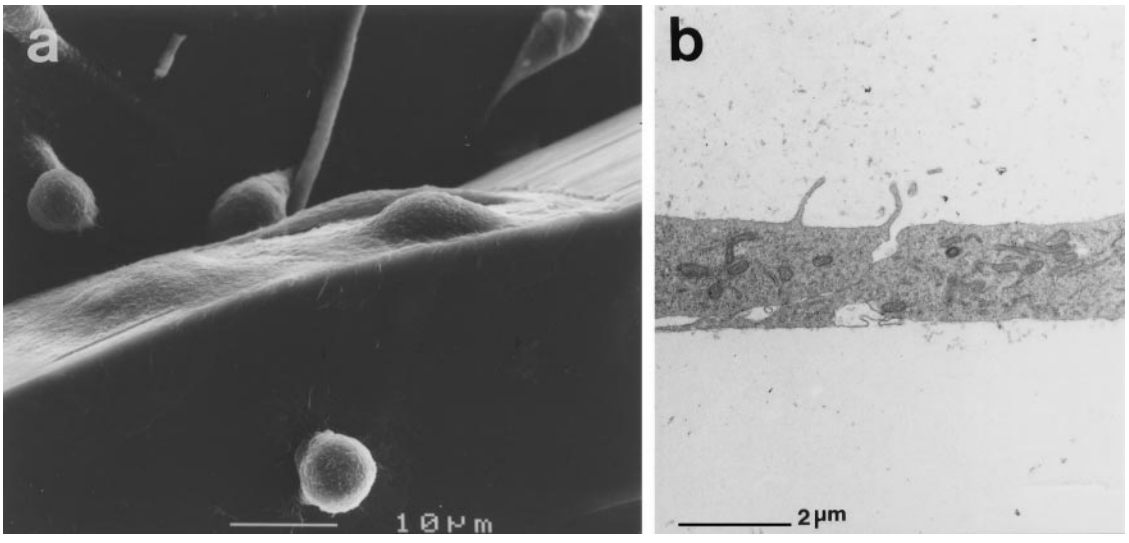

FIG. 8. Scanning (a) and transmission (b) electron micrographs of A6 cells spread on the {0*kl*} faces of calcium-(*R*,*S*)-tartrate trihydrate crystals, 3 (a) and 24 h (b) after plating.

in that it leaves the chemical formula of the compound untouched. The stereochemistry of the whole molecule is, however, not related by symmetry to the two mentioned above. The structure of the crystal is thus bound to be different, and indeed it is. The study of this crystal consequently allowed new factors that have important effects on the development of cell adhesion to be discovered and studied.

The new observations relate especially to the adhesive behavior on the large plate faces {100} of the crystal and may be accounted for in light of two main factors: the presence of water molecules bound to the substrate surface and the topographical aspects of the same surfaces. It was observed that, whereas surface-bound water is, in itself, not compatible with cell spreading and long-term survival, it does allow cell attachment and motility. Cell–cell contacts that compensate for the lack of matrix attachment and allow cell survival consequently develop. In addition, topographical irregularities, originating from these surfaces, which are accompanied by drastic structural differences, promote cell adhesion and spreading and stimulate penetration of cell processes into the crystal bulk. We will offer an explanation for the interplay between attachment, spreading, aggregation and penetration, based on the molecular structure of the various surfaces.

A6 cells attach to the {100} faces of the calcium-(*R*,*S*)-tartrate trihydrate crystals via a foot-like process without forming focal contacts and actin bundles and without undergoing spreading. Time-lapse cinematography indicated that cells attached to the {100} faces are highly motile and have a tendency to undergo clustering. The molecular structure of these faces is such that they are covered, at any given time, by a continuous layer of water molecules. These molecules differ from regular hydration water in that they are bound to the surface at crystallographically defined positions and with an energy higher than the average hydration energy/molecule (Vogler, 1998). Although they may be rapidly exchanging with bulk water, the overwhelming concentration of water in aqueous solutions will always favor full occupancy of the surface sites.

It is thus clear that a cell, when approaching the surface, is confronted with a layer of structured water. The approaching cell has then, at least in theory, a number of options: (1) The cell might not distinguish between the structured water molecules on the crystal surface and bulk water and therefore will not attach. (2) The cell may distinguish and favor the structured water on the crystal surface and attach to it. (3) The cell may be able to directly sense the groups underlying the water layer and attach to them. (4) The cell may loosely bind to the structured water layer and "hang on" there long enough to locally remove water molecules and directly adhere to the underlying layer.

The different cellular and molecular orders of magnitude should be pinpointed here in the dimensions of size, time, and energy, relative to the attachment process. The single molecular moieties that participate in one binding event are on the order of angstroms in size; the tips of the cellular protrusion are on the order of fractions of micrometers. The time-scale of the formation of one single chemical interaction, such as the exchange of hydrogen bonds between water molecules, is on the order of picoseconds. Cell filopodia establish and retract their contacts with the matrix within seconds. It is thus

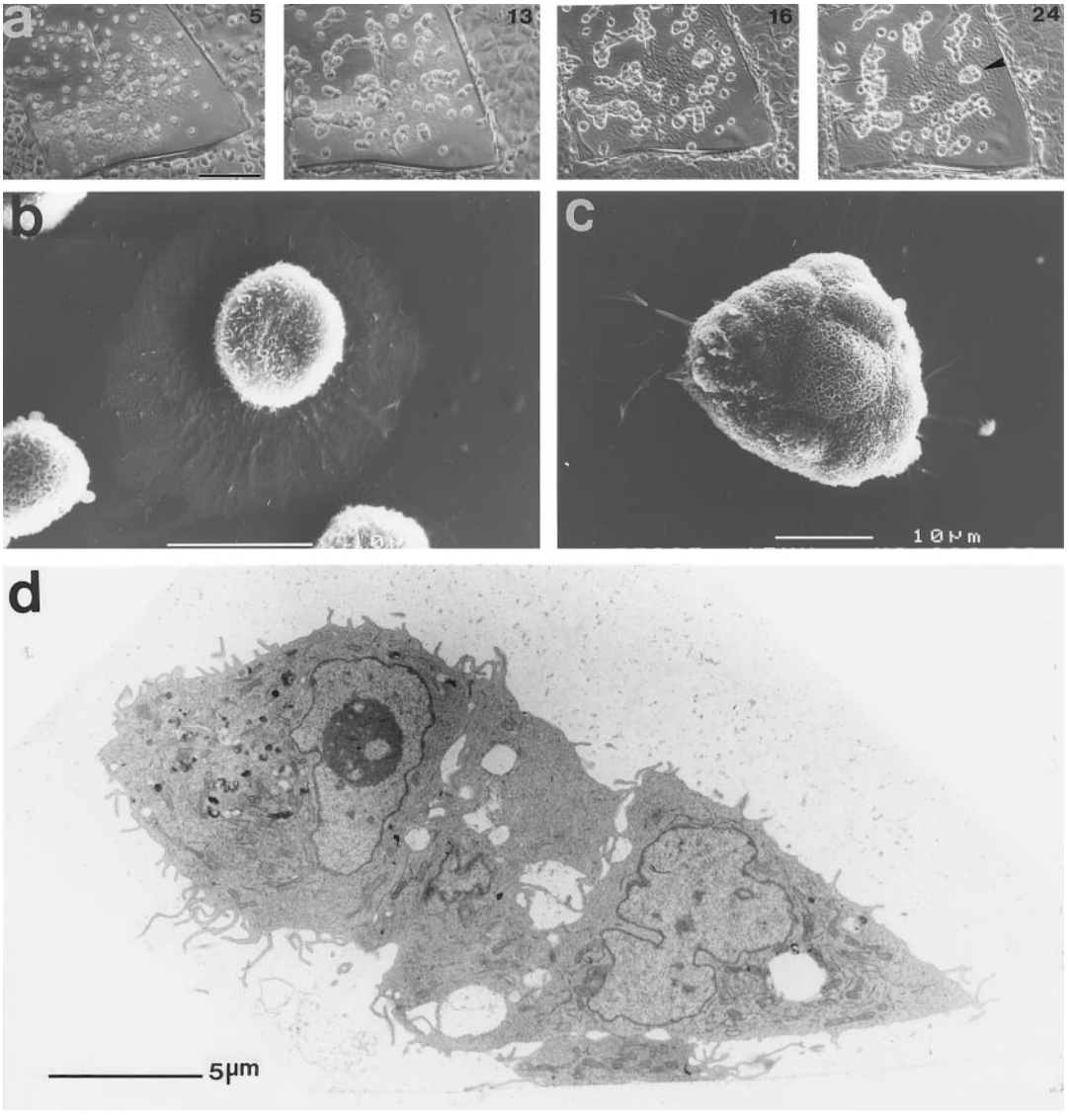

FIG. 9. (a) Time-lapse microscopic tracing of A6 cells on (100) faces of a calcium-(*R*,*S*)-tartrate trihydrate crystal photographed at 5, 13, 16, and 24 h after plating. Bar, 100 µm. Note the progressive cell aggregation (marked with an arrow). (b,c) Scanning electron micrographs of cells on the {100} faces 6 (b) and 24 h (c) after plating. (d) Transmission electron micrograph of a multicellular aggregate of A6 cells on the {100} face 24 h after plating.

reasonable to assume that each protrusion will establish a number of chemical interactions, acting cooperatively in the initial attachment to the surface (Sackmann, 1996). The cellular protrusion may, in turn, extend and flatten, increasing the number of interactions. In addition, long-range cooperativity due to the extension of adhesion to new membrane protrusions may also contribute to the strength of attachment of the cells to the surface.

We know that the number of cells initially attached per unit area of the plate faces is the lowest relative to the other two face types and the culture dish. The percentage of encounters evolving into binding to this crystal face is thus the lowest. This suggests that an abundance of bulk water reduces the probability of effective interaction with surface-bound water and/or that the binding energy developed in the encounter is not always sufficient to hold the cell attached to the surface.

It is still not clear whether the short- and long-term (minutes–hours) association with the surface occurs via direct binding to surface water molecules or involves active removal of water molecules to allow cell interaction with the underlying layer. The observed behavior is, however, consistent with previous data, showing direct binding (not mediated

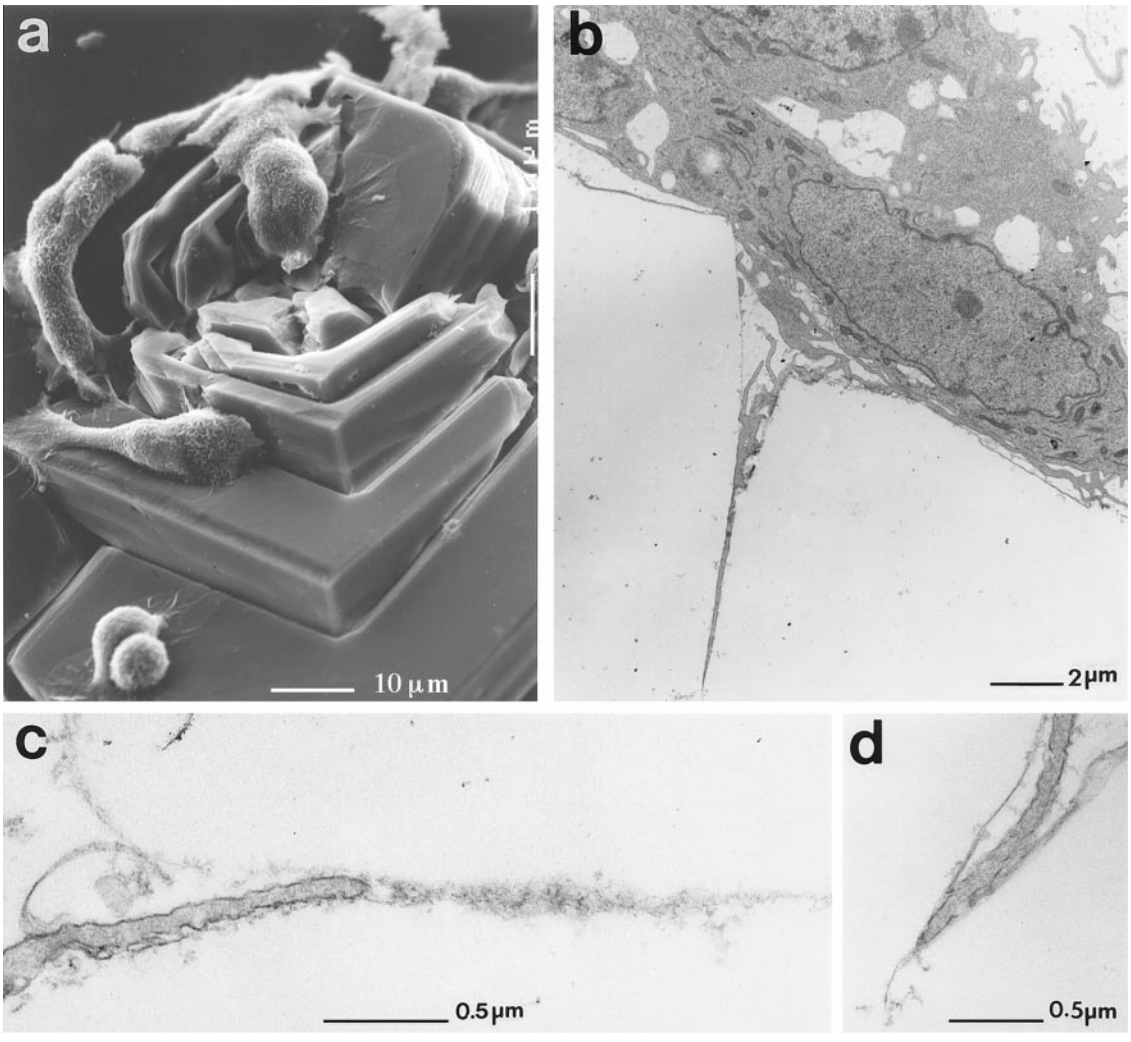

FIG. 10. (a) Scanning electron micrograph of A6 cells attached to a spiral dislocation emerging from the {100} face, 24 h after plating. (b–d) Transmission electron micrographs of cell extensions penetrating inside crystal dislocations, 24 h after plating.

through exogenous proteins) of cells to surfaces that are decorated with water and hydroxyl groups similar in their binding affinity to water molecules.

The lack of cell spreading on the {100} faces is consistent with the finding that matrix proteins (such as fibronectin) do not adsorb on this surface. The inability of water-bound surfaces to adsorb proteins has been previously reported by Hanein *et al.* (1993a), who compared fibronectin adsorption to a series of crystal surfaces with increasing amounts of surface-bound water. It was shown that the extent of adsorption was inversely proportional to the extent of coverage of the surface by bound water, reaching levels below detection on surfaces that are completely covered by water molecules. The most probable explanation of this effect is based on the relatively high energy required to remove the water of hydration of both protein and crystal surface, before the protein can adsorb.

The fact that cells can bind to the same surfaces where proteins cannot adsorb indicates a different binding mechanism. This may be attributed to the higher cooperativity of cellular interactions, relative to a protein, due to the large difference in dimensions. Alternatively, it may be due to the specific nature of the binding groups on the cell surface, different from those on proteins. To further develop focal contacts and spread on the surface, the cells need to bind to substrate-attached matrix proteins, leading to integrin-mediated adhesion. In the absence of protein binding to the surface, integrin-mediated adhesion cannot occur. The cell may, however, remain motile. The cells attached to the {100} faces are bound through an extended network of hydrogen bonds to rapidly exchanging molecules. The locomotion in this case involves establishment of new bonds while retracting others, in a highly cooperative process. The removal of a number of hydro-

gen bonds while forming an equal number of other, perfectly equivalent, bonds is not expected to cost in terms of energy. In this context, it is worth noting that many highly motile cells (i.e., neutrophils) do not form extensive adhesions and that large focal contacts are more characteristic of stationary cells.

The long-term behavior of A6 cells on the {100} faces provided some additional insight into the involvement of cell–matrix and cell–cell adhesion in the prevention of apoptosis. Single A6 cells attached to the {100} faces for extended periods (>24 h) cannot survive and apparently undergo apoptosis. This is consistent with the current view that integrin-mediated interactions trigger signaling events in epithelial cells that are essential for cell survival (Hanein *et al.*, 1996; Frisch and Francis, 1994; Frisch and Ruoslahti, 1997; Aoshiba *et al.*, 1997; Hermiston and Gordon, 1995; Kataoka *et al.*, 1993; Lindhout *et al.*, 1993; Peluso, 1997; Peluso *et al.*, 1996; Raff, 1992). However, it is shown here that cell–cell interactions can substitute for cell–matrix adhesions in preventing apoptosis. Such interactions can take place on the {100} faces since the attached cells on these faces remain highly motile and tend to form surface-attached multicellular aggregates. As shown here, over 80% of the cells are viable, suggesting that intercellular interactions can generate "survival signals" and rescue the cells.

In contrast to the behavior on the {100} faces, cell interactions with the smooth lateral {011} faces of the crystals are relatively rapid, as deduced from the numerous traces of detached cells found on these faces following only a few minutes of incubation. It is conceivable that while the initial interactions of the cells with the {011} faces are rather rapid, they are not sufficiently robust and stable to retain the cells attached. It is only after at least 5–15 min of incubation that multiple local interactions are formed, tethering the cells to the crystal surface. Despite this delay between formation of initial contacts and establishment of stable adhesions, the overall rate of cell attachment to the {011} crystal faces is still higher than the rate of attachment to the other faces of the crystal or even to the tissue culture dish. The attached cells are, however, not motile, do not spread, do not form focal contacts and stress fibers, and do not survive following prolonged incubation, despite the presence of fibronectin on the surface. This behavior is reminiscent of that observed on the hydroxylated surfaces of calcium-(*R*,*R*)-tartrate tetrahydrate crystals. It was attributed to the high density of binding groups on this crystal surface, leading to what appears to be a cell "paralysis." Interestingly, the structure of the relevant faces of calcium-(*R*,*R*)-tartrate is remarkably similar to that of the {011} faces of calcium-(*R*,*S*)-tartrate. Both crystal faces expose rows of hydroxyl groups intercalated by rows of water molecules. The third isomer, {*S*,*S*}, which is the mirror image of {*R*,*R*} in its molecular, crystalline, and surface structure, however, did not bind cells to its hydroxylated faces. This indicates that the chemical nature of the exposed groups per se is not sufficient to account for the attachment behavior and that recognition of the faces by the cells is stereoselective.

The evidence collected on the three isomers, considered together, strengthens the hypotheses advanced previously and leads to a number of tentative conclusions: (i) Cell attachment is induced by the groups exposed at the surface, no matter what is immediately underlying it. Thus different faces may have different attachment behavior, even though they are composed of the same molecules. (ii) Surfaces exposing hydroxylated carbons are particularly inducive to attachment as already observed on different artificial substrates (Curtis *et al.*, 1986). Thus the (*R*,*R*) and (*R*,*S*) isomers behave analogously, even though the structure is not the same. (iii) Cell attachment occurs through cooperative interactions of many groups whose individual binding is stereospecific. Thus, the cells attach to the hydroxylated {011} faces of both the (*R*,*R*) and the (*R*,*S*) isomers, but not to the same faces of the (*S*,*S*) isomer. The attachment on the {*R*,*S*} isomer appears to differ from that on the {*R*,*R*} quantitatively, rather than qualitatively. It is tempting to suggest that the intensity of the binding is regulated by the density of the groups of the correct stereochemistry, *R*. This "dilution" of binding groups might explain why the attachment is less massive on the (*R*,*S*) crystal. It appears, however, that on both (*R*,*R*) and (*R*,*S*) crystal faces the density of the binding groups is still high enough to prevent interaction via specific ECM receptors, which is a prerequisite for focal contact formation and cell survival.

It is appropriate to note here that while apoptosis of cells on both the {011} faces and the {100} faces appears to be related to failure to interact with the ECM, the mechanism underlying this failure is distinctly different on the two faces. On the {100} water-bound faces, matrix proteins do not easily adsorb and thus are not available to the cells. In contrast, on the {011} faces, matrix proteins do adsorb but the cells form initial firm binding that apparently prevents them from interacting with the matrix proteins.

Cell spreading and focal contact formation occur only on the faces of the {0*kl*} family. At the submicrometer level, these faces are rough. At the molecular level, they display a broad range of surface organizations. They are composed of segments of stable crystallographic faces whose combination re-

sults in a given average index $\{0kl\}$, with each segment, and thus each crystallographic motif, repeating in an ordered sequence. On these faces, proteins, including fibronectin, do adsorb. Proteins are known to adsorb preferentially at crystal imperfections and on surfaces decorated by molecular steps or kinks, namely rough surfaces. This is due both to their large surface area and to incomplete formation of crystal layers. Here a wide variety of functional groups, which would be buried in a complete layer, are left exposed and free to interact with foreign adsorbates.

Concomitant to protein adsorption, the cells spread, flatten extensively on the $\{0kl\}$ faces, and within less than a day completely cover the surface. They form vinculin-rich focal contacts and assemble stress fibers. There is ample evidence that the formation of these structures depends on RGD-mediated interactions with the appropriate integrins on the cell surface and on cell contractility (Bershadsky *et al.*, 1996; Chrzanowska-Wodnicka and Burridge, 1996). Following spreading on the $\{0kl\}$ surface, the cells remain vital even after prolonged incubation in culture and show no tendency to undergo apoptosis.

Apparently, combinations of the chemical nature and topography of the $\{0kl\}$ faces provide the essential conditions for focal contact, stress fiber formation, and survival. We cannot define at this stage whether this cell behavior is linked to protein adsorption or directly to the molecular structure of the surface and/or its macroscopic topography. Within the latter parameters, it is also unclear whether the mixed character of the surface itself or the contribution of each of the structural motifs separately (as in a "mosaic" structure) is promoting the adhesion and spreading of the cells.

Whichever the explanation for the cell behavior on the $\{0kl\}$ faces is, it is consistent with the cell behavior on the macroscopic imperfections that emerge from the large plate face of the crystal. Here, cells extend long protrusions deep into the crystal, along surfaces that are of the $\{0kl\}$ type. Active spreading of these extensions into these sites is apparently sufficient to induce cell survival, although the overall morphology of the cell body, which is mostly confronting the plate face, remains spherical. This indicates that the cell, while minimizing its contact area with the $\{100\}$ surface, maximizes its contact area (even only by a protrusion) with other, more congenial surfaces and survives. The penetration is active and the cells appear to expand the original size of existing cracks and push their way deep into the crystal. It is yet to be determined whether the cell itself applies the force to widen the crack or rather induces local dissolution of the crystal.

Crystals have been used here as adhesive surface models for the characterization of specific molecular events involved in various stages of the adhesion process. We note, however, that they are also involved in contacts with cells in a number of physiological and pathological conditions. For example, the bone-resorbing activity of osteoclasts appears to be triggered by the presence of apatite crystals in bone (Chambers, 1988). Macrophages and endothelial cells actively interact with cholesterol crystals in atherosclerotic plaques (Guyton, 1994) and adhesion of calcium oxalate and other crystals to the epithelial layer lining the kidney is associated with kidney stone formation. In the latter system, preference for adhesion of the crystals to cell monolayers through one crystal face was observed (Lieske *et al.*, 1996). The determination of the importance of structural parameters of solid substrates in cell adhesion may thus have direct relevance to biological situations.

We thank Helena Sabanay for her expert help with the transmission electron microscopy. We thank Dr. Linda Shimon for her help in the determination of the morphology of the calcium-(*R*,*S*)-tartrate tetrahydrate crystals. We thank Amir Aharoni for his contribution to an early stage of this work. L.A. is the incumbent of the Dorothy and Patrick Gorman professorial chair. B.G. is the incumbent of the E. Neter Chair in Tumor and Cell Biology. This work was supported by the Israel Science Foundation administrated by the Israel Academy of Sciences and Humanities.

REFERENCES

Aoshiba, K., Rennard, S. I., and Spurzem, J. R. (1997) Cell–matrix and cell–cell interactions modulate apoptosis of bronchial epithelial cells, *Am. J. Physiol.* **272,** L28–L37.

Bershadsky, A., Chausovsky, A., Becker, E., Lyubimova, A., and Geiger, B. (1996) Involvement of microtubules in the control of adhesion-dependent signal transduction, *Curr. Biol.* **6,** 1279–1289.

Butcher, E. C., and Picker, L. J. (1996) Lymphocyte homing and homeostasis, *Science* **272**(5258), 60–66.

Chambers, T. J. (1988) The regulation of osteoclastic development and function, *in* Cell and Molecular Biology of Vertebrate Hard Tissues. Ciba Foundation Symposium, Vol. 136, pp.92–107. Wiley, New York.

Chrzanowska-Wodnicka, M., and Burridge, K. (1996) Rho-stimulated contractility drives the formation of stress fibers and focal adhesion, *J. Cell. Biol.* **133,** 1403–1415.

Curtis, A. S. G., Forrester, J. V., and Clark, P. (1986) Substrate hydroxylation and cell adhesion, *J. Cell Sci.* **86,** 9–24.

DeVries, A. J., and Kroon, J. (1984) Conformational aspects of *meso*-tartaric acid. VII. Structure of calcium *meso*-tartrate trihydrate, *Acta Crystallogr. Sect. C* **40,** 1542–1544.

Frisch, S. M., and Francis, H. (1994) Disruption of epithelial cell–matrix interactions induces apoptosis, *J. Cell Biol.* **124,** 619–626.

Frisch, S. M., and Ruoslahti, E. (1997) Integrins and anoikis, *Curr. Opin. Cell Biol.* **9**(5), 701–6.

Geiger, B., Yehuda, L. S., and Bershadsky, A. D. (1995) Molecular interactions in the submembrane plaque of cell–cell and cell–matrix adhesions, *Acta Anat. Basel* **154**(1), 46–62.

Guyton, J. R. (1994) The arterial wall and the atherosclerotic lesion, *Curr. Opin. Lipidol.* **5,** 376–381.

Hanein, D., Geiger, B., and Addadi, L. (1993a) Fibronectin adsorption to surfaces of hydrated crystals: An analysis of the importance of bound water in protein–substrate interactions, *Langmuir* **9,** 1058–1065.

Hanein, D., Geiger, B., and Addadi, L. (1994) Differential adhesion of cells to enantiomorphous crystal surfaces, *Science* **263**(5152), 1413–6.

Hanein, D., Geiger, B., and Addadi, L. (1995) Cell adhesion to crystal surfaces: A model for initial stages in the attachment of cells to solid substrates, *Cells Mater.* **5**(2), 197–210.

Hanein, D., Sabanay, H., Addadi, L., and Geiger, B. (1993b) Selective interactions of cells with crystal surfaces. Implications for the mechanism of cell adhesion, *J. Cell Sci.* **104,** 257–288.

Hanein, D., Yarden, A., Sabanay, H., Addadi, L., and Geiger, B. (1996) Cell adhesion to crystal surfaces. Adhesion-induced physiological cell death, *Cell Adhes. Commun.* **4,** 341–354.

Hermiston, M. L., and Gordon, J. I. (1995) In vivo analysis of cadherin function in the mouse intestinal epithelium: Essential roles in adhesion, maintenance of differentiation, and regulation of programmed cell death, *J. Cell. Biol.* **129**(2), 489–506.

Kansas, G. S. (1996) Selectins and their ligands: Current concepts and controversies, *Blood* **88**(9), 3259–87.

Kataoka, S., Naito, M., Fujita, N., Ishii, H., Ishii, S., Yamori, T., Nakajima, M., and Tsuruo, T. (1993) Control of apoptosis and growth of malignant T lymphoma cells by lymph node stromal cells, *Exp. Cell Res.* **207**(2), 271–6.

Lieske, J. C., Toback, F. G., and Deganallo, S. (1996) Face-selective adhesion of calcium oxalate dihydrate crystals to renal epithelial cells, *Calcif. Tissue Int.* **58,** 195–200.

Lindhout, E., Mevissen, M. L., Kwekkeboom, J., Tager, J. M., and de Groot, C. (1993) Direct evidence that human follicular dendritic cells (FDC) rescue germinal centre B cells from death by apoptosis, *Clin. Exp. Immunol.* **91**(2), 330–6.

Peluso, J. J. (1997) Putative mechanism through which N-cadherin-mediated cell contact maintains calcium homeostasis and thereby prevents ovarian cells from undergoing apoptosis, *Biochem. Pharmacol.* **54**(8), 847–53.

Peluso, J. J., Pappalardo, A., and Trolice, M. P. (1996) N-cadherin-mediated cell contact inhibits granulosa cell apoptosis in a progesterone-independent manner, *Endocrinology* **137**(4), 1196–203.

Raff, M. C. (1992) Social controls on cell survival and cell death, *Nature* **356**(6368), 397–400.

Sackmann, E. (1996) Supported membranes: Scientific and practical applications, *Science* **271**(5245), 43–48.

Springer, T. A. (1994) Traffic signals for lymphocyte recirculation and leukocyte emigration: The multistep paradigm, *Cell* **76**(2), 301–14.

Takeichi, M. (1995) Morphogenetic roles of classic cadherins, *Curr. Opin. Cell. Biol.* **7**(5), 619–27.

Vogler, E. A. (1998) Structure and reactivity of water at biomaterial surfaces, *Adv. Colloid Interface Sci.* **74,** 69–117.

Yamada, K. M., and Geiger, B. (1997) Molecular interactions in cell adhesion complexes, *Curr. Opin. Cell Biol.* **9**(1), 76–85.